

Hands-on lab steps of practical course: Vibrating wire monitors and beam profile measurements

S.G. Arutunian, A.V. Margaryan, G.V. Mirzoyan

Practical course setup presents the main units of beam profile station based on Vibrating Wire Monitor (VWM). Beam is modelled by laser.

Test-bench of the VWM station

Vibrating wire monitors were originally designed for accelerator beam profiling. Our test-bench uses a laser instead of an accelerator beam, which allows us to perform experiments to investigate the process of beam profiling (Fig. 1).

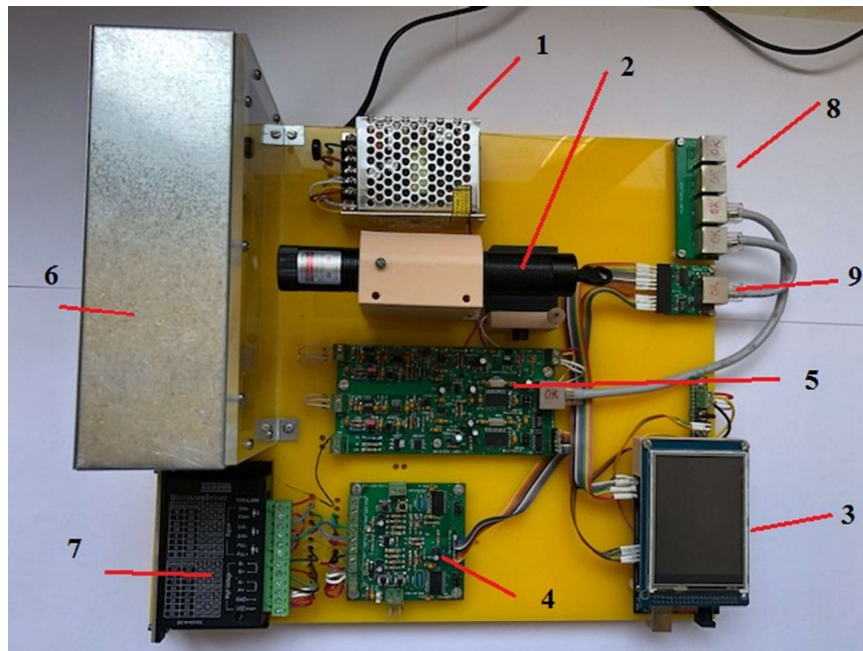


Figure 1. Power supply (1), laser (2), Arduino Mega 2560 (3), stepper motor control board (CTRL-2XTB) (4), wire autogeneration board (VW-MIX_U) (5), vibrating wire monitor (VWM) (6), line actuator based on stepper motor (TB6600) (7), Network hub (8), interface Arduino to PC (9).

The power supply converts the 50 Hz and 220 V to a DC 12 V, which is used for the boards (4), (5) and the Arduino (3). The laser has a power of <math><100\text{ mW}</math> and radiates light with a wavelength of 532 nm ($\pm 10\text{ nm}</math>). Laser brightness is varied by DC voltage. The CTRL-2XTB board is designed to operate the motor CTRL-2XTB. VW-MIX_U board provides the wire frequency autogeneration and the recording of the wires oscillation frequency.$

We use two ways of presenting the obtained results: The first way is by the application LabRab on PC display and the second by display of Arduino.

The VWM is housed in a box to eliminate airflow noise.

TB6600 Arduino Stepper Motor Driver is an easy-to-use professional stepper motor driver, which could control a two-phase stepping motor. It is compatible with Arduino and other microcontrollers that can output a 5 V digital pulse signal.

One side of the VWM box is covered by plexiglass. By the hole on it the laser beam falls onto the vibrating wire.

The VWM is moved perpendicular to the laser beam by a stepper motor. When wires cross the beam, its frequencies decrease due to the loosening of the wires tension.

The schematic diagram of the test bench is showed in Fig. 2

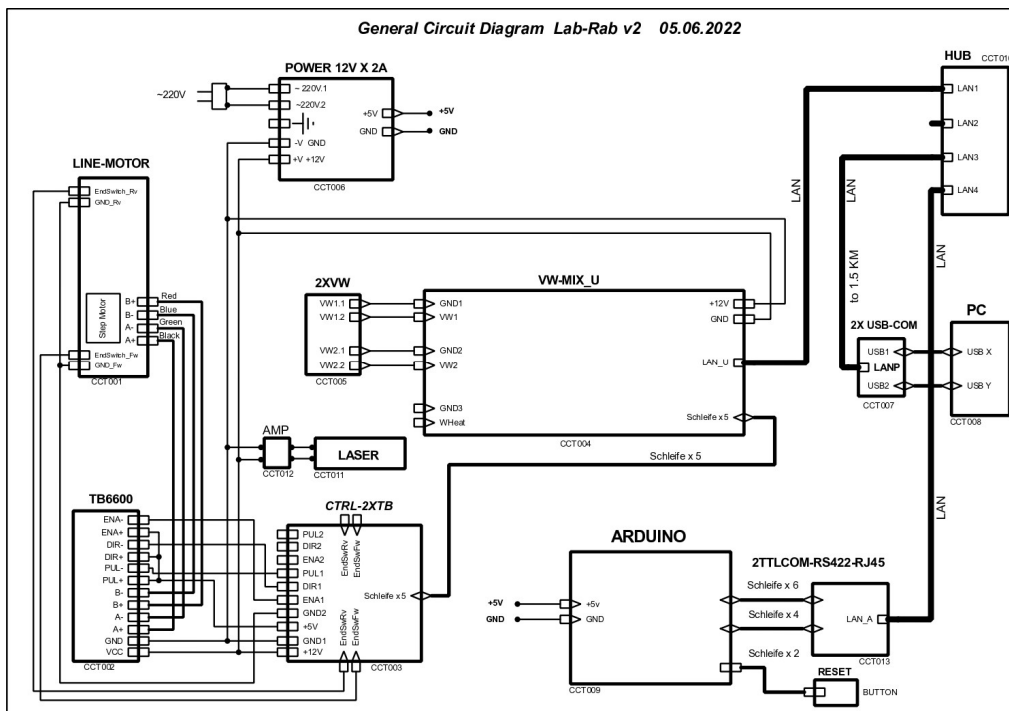


Figure 2. Schematic diagram of the test bench.

Vibrating wire monitor

The monitor used in test-bench has two wires, that is, we have the opportunity to make measurements for two wires with similar parameters.

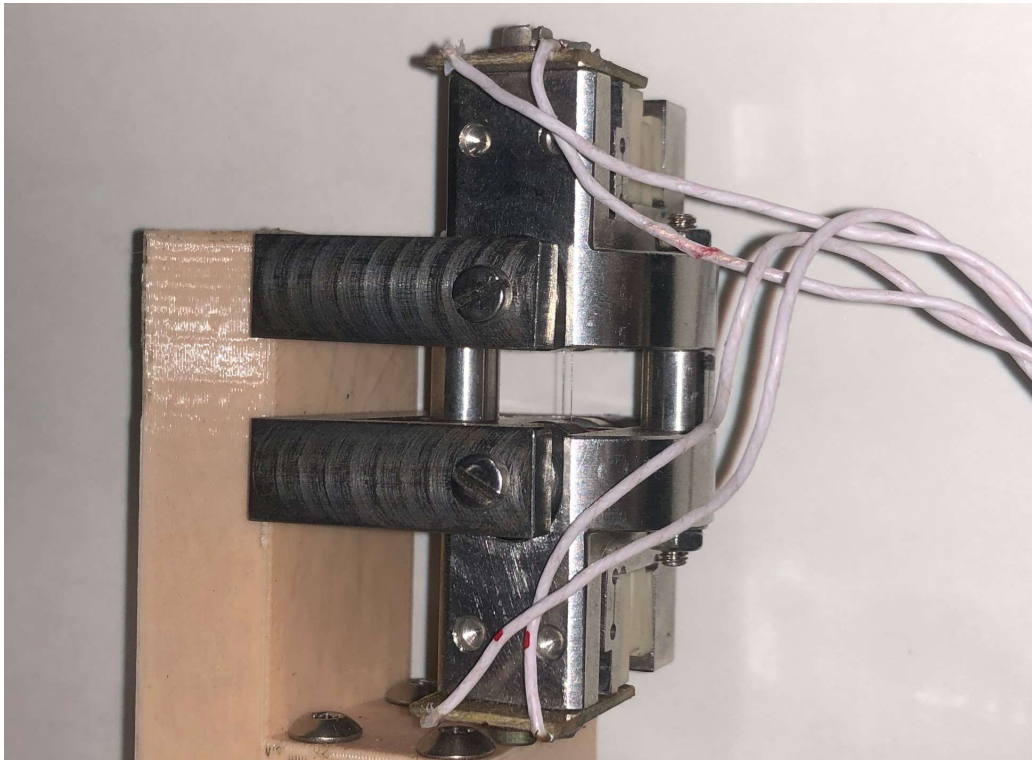


Figure 3. Two wire VWM.

Fig. 3 shows a vibrating wire monitor whose parameters are presented below.

VWM parameters

| | |
|------------------------------------|-----------------------|
| Number of wires | 2 |
| Wire material; | Stainless steel, A316 |
| Wire length; | 36 mm |
| Wire diameter; | 100 μm |
| The distance between the two wires | 1 mm |
| Base material; | Steel |
| Aperture; | 6 mm |

Other parameters (see VWM_choice_Rev4.doc and Note to VWM_Choice_Rev3 VWM_Choice_Rev4.doc):

| | |
|--------------------------------------------|------|
| Wire frequency dependence on T, Hz/K; | 27 |
| Wire T dependence on deposited power, K/W; | 4531 |
| Response time (in air), s; | 4.2 |

Wire T shifts limits, K; min 0.4E-03 / max 80

Wire deposited power limits, W; min 8E-08 / 1.1E-02

Generation of wire oscillations is organized on the second harmonics.

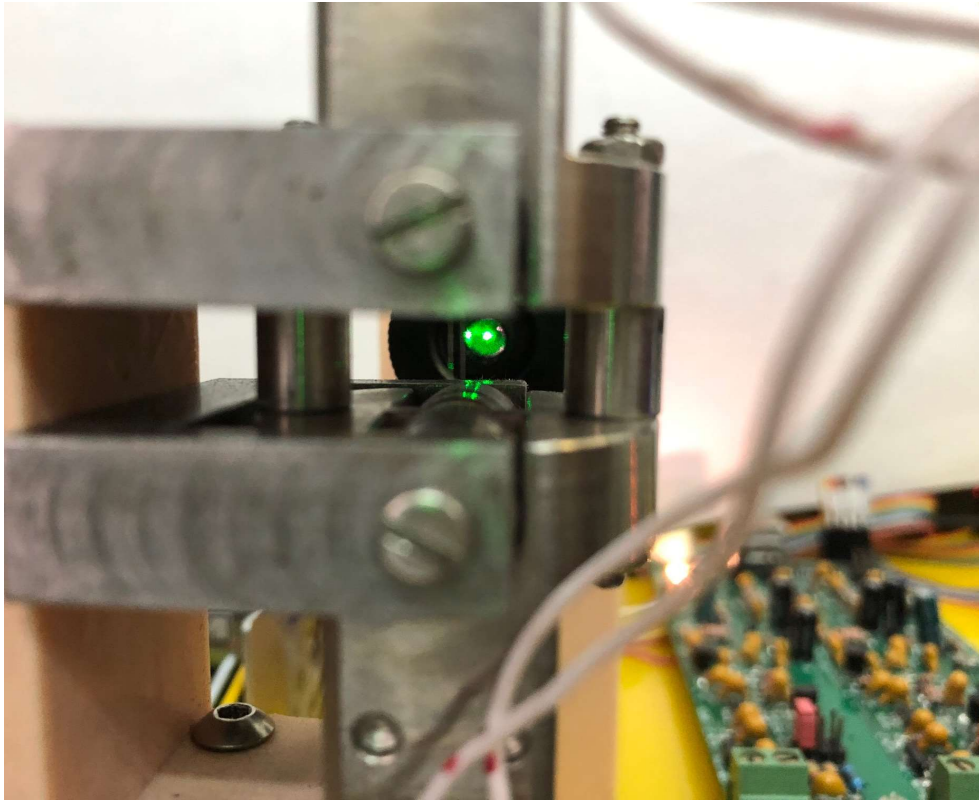


Figure 4. Laser beam falling on the wire of VWM.

Figure 4 shows a vibrating wire monitor on which the laser beam falls. Wire heats up by absorbing light photons leads to decrease of the wire oscillation frequency.

We have the ability to see the data from the wire with an oscilloscope connected to the autogeneration board (Fig. 5).

| | |
|-------------------------|----------|
| Accuracy, mm | 0.05 |
| Max horizontal load, kg | 3 |
| Item diameter, mm | 30 |
| Material | Aluminum |

Setup objectives

- Familiarization with the principle of operation of vibrating wire sensors/monitors and characteristic parameters (length between VWM clamps, wire diameter and material, permanent magnets polarization in magnet poles, aperture).
- Familiarization with R&S®RTB2004 Digital Oscilloscope and its adaptation to experimental stand and check proper generation of wire oscillation.
- Usage of the application program LabRab for wire frequency measurement and data acquisition.
- Carrying out the experiment of scan the Laser beam by means of VWM.
- Process the experimental data and recover beam profile.

Equipment and software

- Assembled vibrating wire monitor.
- Vibrating wire boards
- 12 V power supply.
- Linear actuator with stepper motor
- Semiconductor laser (Laser 303g, 2000 mW green laser, 532 nm)
- R&S®RTB2004 Digital Oscilloscope.
- Application program LabRab (Appendix 2)

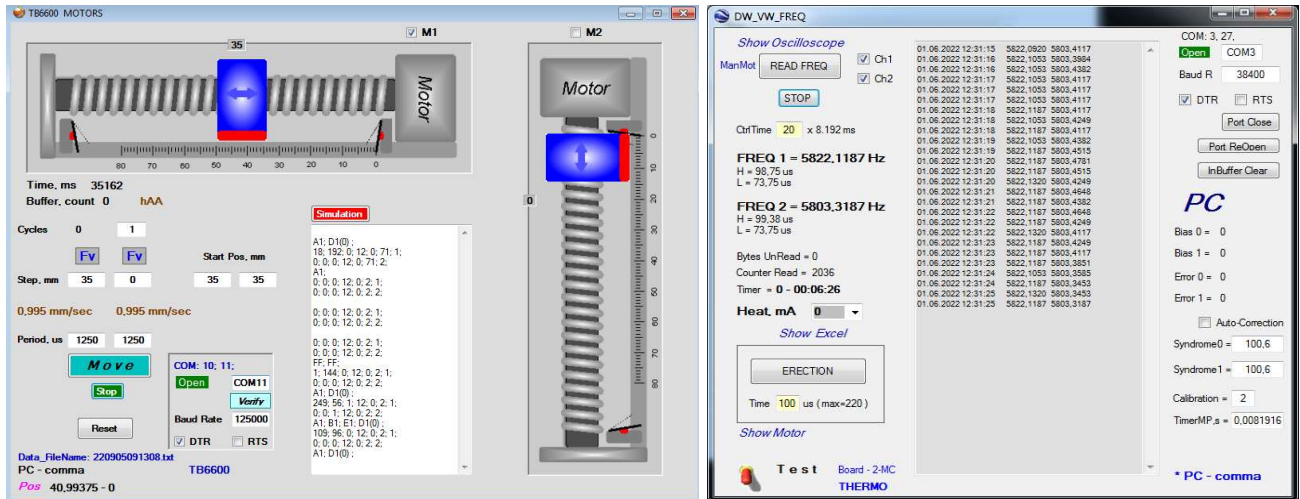
Description and procedures

- Prepare test-bench wiring
- Wire the oscilloscope as presented in Fig.5.
- Check the wire oscillation generation quality and investigate of generation process, take corresponding graphs of oscilloscope.
- SWITCH ON LASER

Soft LabRab

After activating the application
 LabRab\AshSoft\Soft\VB_exe\VB_Ash_VW_FREQ_v20MTherm_2xMotors_v3\VB_Ash_VW_FREQ\

B_Ash_VW_FREQ_v2_2xMotors\VB_Ash_VW_FREQ_v2_2xMotors.exe, two programs are opened: DW_VW_FREQ and RB6000 MOTORS. DW_VW_FREQ is responsible for recording and saving the measurements made, and RB6000 MOTORS is responsible for motor operation and for recording motor position according to time of frequency measurements.



a)

b)

Figure 7. a) Program RB6000 MOTORS b) program DW_VW_FREQ

With the RB6000 MOTORS program, it is possible to set the number of cycles (each cycle represent one scan forward and back), the speed and the coordinate where the monitor should stop during one cycle. First we will find the coordinates where the laser is located by set a wide scan and analysis of frequency data. After that we set the initial position of scan (parameter Start Pos, mm) and depth of scan (parameter Step, mm).

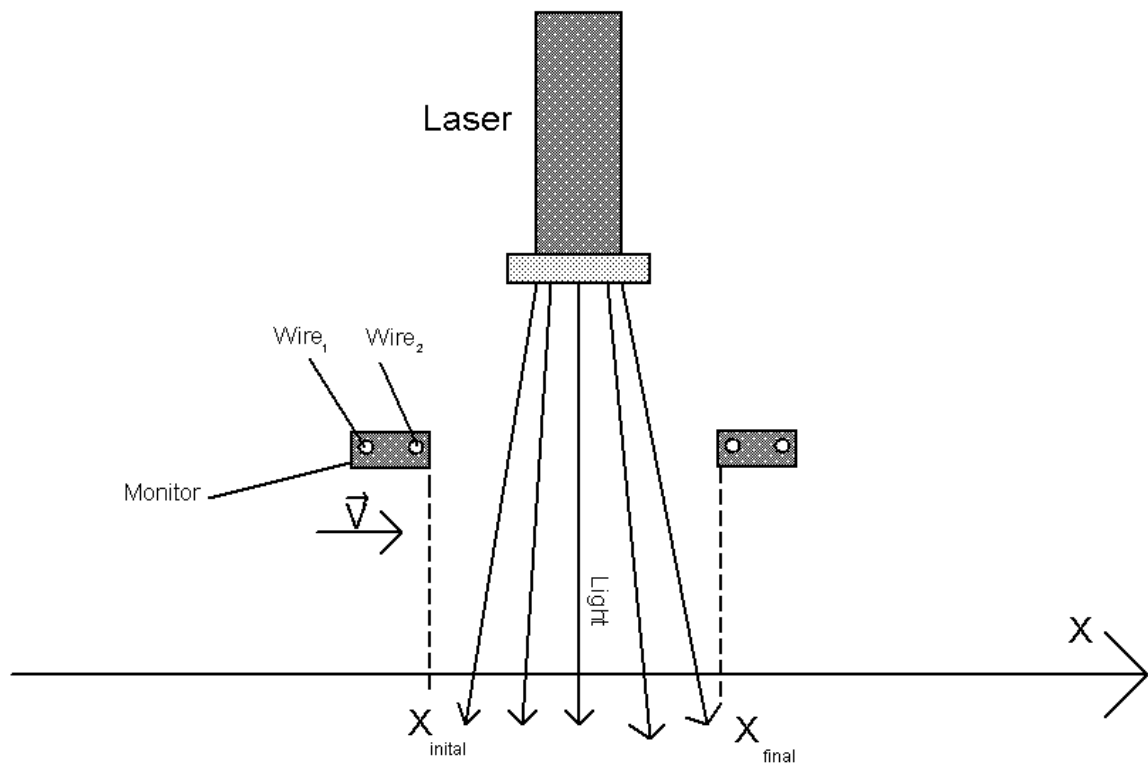


Fig 8. Selection of position of monitor

In the next step we will define these coordinates and make measurements.

Then in program DW_VW_FREQ parameter Manual should be switched to Normal. The start of this program simultaneously with RB6000 MOTORS is provided by READ_FREQ key.

The start of the engine operation is given by the Move key, then we will run the DW_VW_FREQ program to make measurements and record it, using the READ_FREQ key.

- Measurements for two wires are performed in parallel, after the measurement it is sent to the computer in the form of 17 bytes, where the information is recorded and a request is sent to perform the next measurement.
- In Fig. 1(item 5), the wire autogeneration board (VW-MIX_U) is designed to adjust the step frequency of the motor, the board generates a signal that rotates the motor screw by one step.
- There is a large step recognition for the stepper motor, after 200 large steps, one complete revolution is made, which moves the motor by 1.25mm
- Accuracy of 4-step motors is 20μm

Recorded data is saved as a Text Document.

More detailed description of Soft is presented in Appendix 1.

Processing of the obtained results

Aim: to get the transverse profile of the laser.

The laser beam profile is reconstructed from the experimental data (file DataTMP).

To study the resulting data, the measurements recorded in the Text Document are downloaded to an Excel file as shown in Figure 8 (sheet Exp):

| | A | B | C | D | E | F | G |
|----|-------------|------------------|----------|----------|---------|---|--------------|
| 1 | Time, s | Date | F1, Hz | F2, Hz | Pos, mm | | per, mks |
| 2 | 0 | 22.08.2022 12:15 | 5821.921 | 5799.279 | 32.235 | | 12500 |
| 3 | 1.122213304 | 22.08.2022 12:15 | 5821.925 | 5799.276 | 32.12 | | per, s |
| 4 | 2.256250647 | 22.08.2022 12:15 | 5821.921 | 5799.259 | 32.005 | | 0.0125 |
| 5 | 3.376222953 | 22.08.2022 12:15 | 5821.925 | 5799.259 | 31.775 | | step/rev, mm |
| 6 | 4.511819786 | 22.08.2022 12:15 | 5821.925 | 5799.274 | 31.775 | | 2 |
| 7 | 5.628006558 | 22.08.2022 12:15 | 5821.927 | 5799.302 | | | step/per, mm |
| 8 | 6.762704881 | 22.08.2022 12:15 | 5821.925 | 5799.294 | 31.4275 | | 0.00125 |
| 9 | 7.899016653 | 22.08.2022 12:15 | 5821.923 | 5799.276 | 31.31 | | v, mm/s |
| 10 | 9.035321386 | 22.08.2022 12:15 | 5821.923 | 5799.253 | 31.1938 | | 0.1 |
| 11 | 10.17034433 | 22.08.2022 12:15 | 5821.927 | 5799.24 | 31.1938 | | |
| 12 | 11.30474824 | 22.08.2022 12:15 | 5821.927 | 5799.252 | 31.0763 | | |
| 13 | 12.42545044 | 22.08.2022 12:15 | 5821.927 | 5799.265 | 30.9613 | | |
| 14 | 13.56141266 | 22.08.2022 12:16 | 5821.927 | 5799.276 | 30.7938 | | |
| 15 | 14.69534443 | 22.08.2022 12:16 | 5821.927 | 5799.261 | 30.7938 | | |
| 16 | 15.83056385 | 22.08.2022 12:16 | 5821.925 | 5799.28 | 30.6775 | | |
| 17 | 16.96620819 | 22.08.2022 12:16 | 5821.925 | 5799.286 | 30.51 | | |
| 18 | 18.10165958 | 22.08.2022 12:16 | 5821.925 | 5799.292 | 30.3925 | | |
| 19 | 19.24249675 | 22.08.2022 12:16 | 5821.925 | 5799.306 | 30.2763 | | |
| 20 | 20.38987627 | 22.08.2022 12:16 | 5821.925 | 5799.305 | 30.1575 | | |

Figure 8. The Excel file is shown, where column *A* represents the time, column *B* represents the date, columns *C* and *D* represent the oscillation frequencies of the first and second wires, respectively, and *E* represents the position of the linear actuator. The main parameters of scan are marked by green.

First we plot frequencies versus time (Fig. 9).

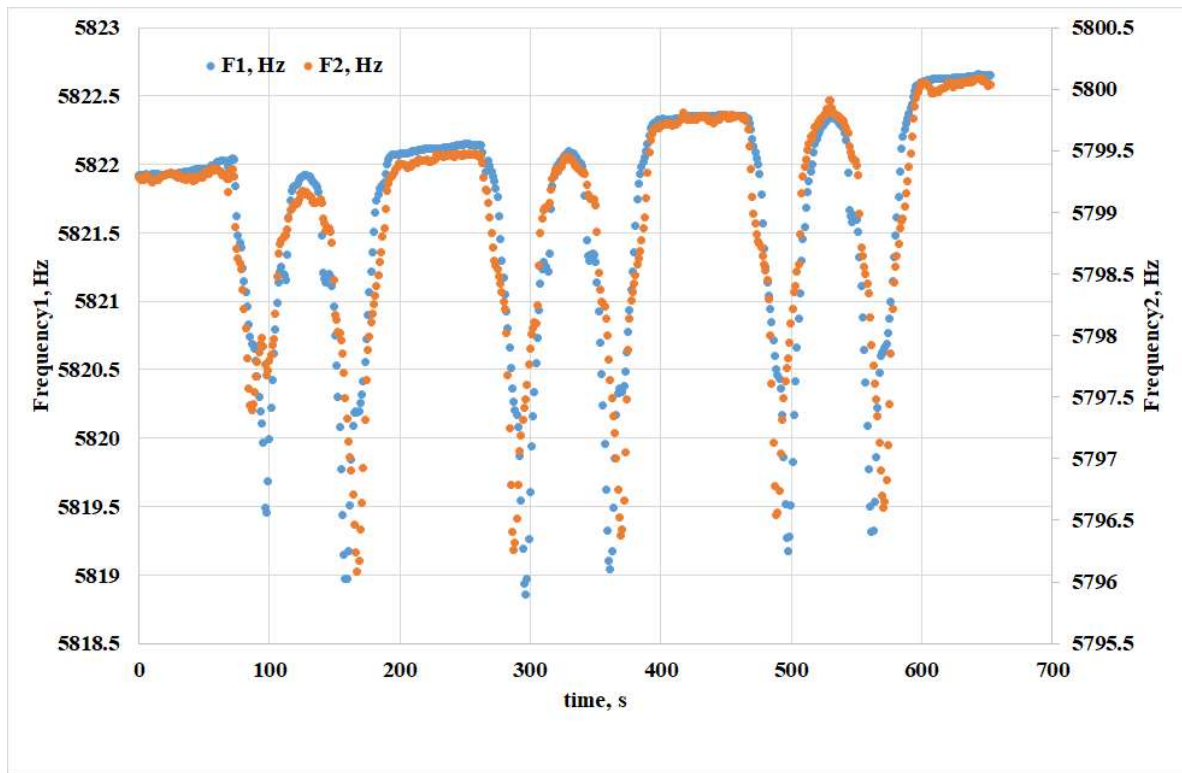


Figure 9. Dependence of the wire oscillation frequencies on time.

Then we present dependence of VWM position and frequency of the 1st wire (Fig. 10).

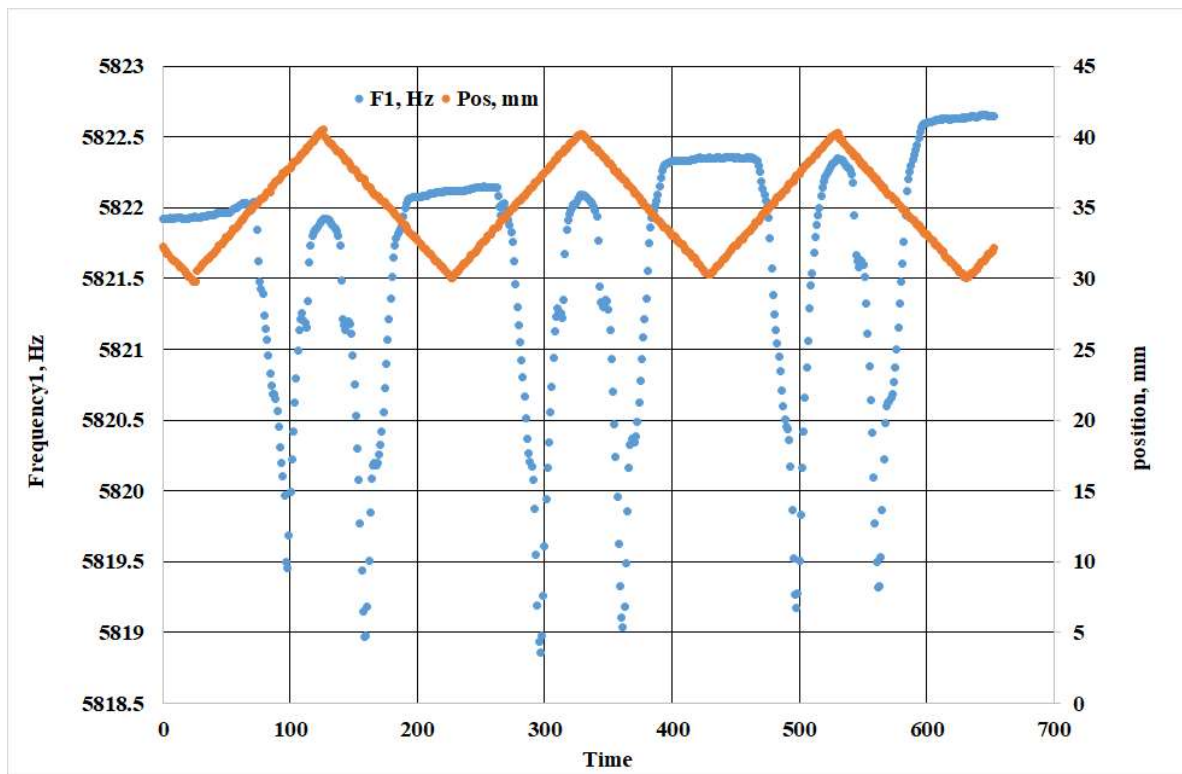


Figure 10. Dependence of frequency and coordinate on time. The coordinate values are depicted in orange and the frequency in blue.

By figs. 9 and 10 we see 3 complete scans. The first scan has unequal frequency drop amplitudes when moving forward and backward, so we discard it. We choose the second scan for analysis (see Fig. 11).

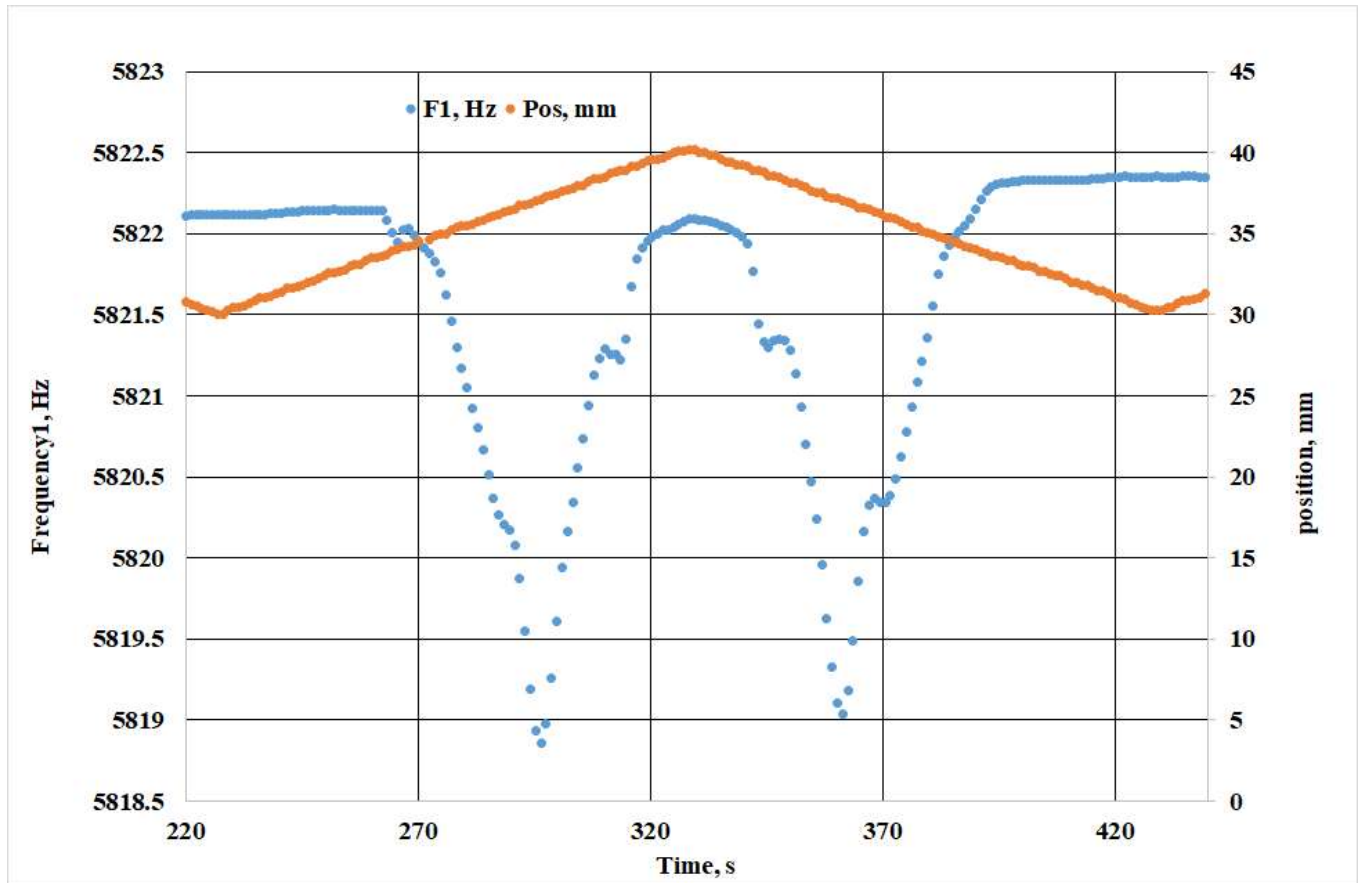


Figure 11. The second scan selected for analysis.

As shown in Figs. 10 and 11 the frequency graph has temporal drift (caused e.g. by ambient temperature change). To exclude the drift we draw a graph of frequency versus time only for tail of process (Fig. 12) where laser beam do not touch the wires.

The Excel program allows us to calculate the linear regression of the selected data points and discriminate the drift. The results are shown in Fig. 12.

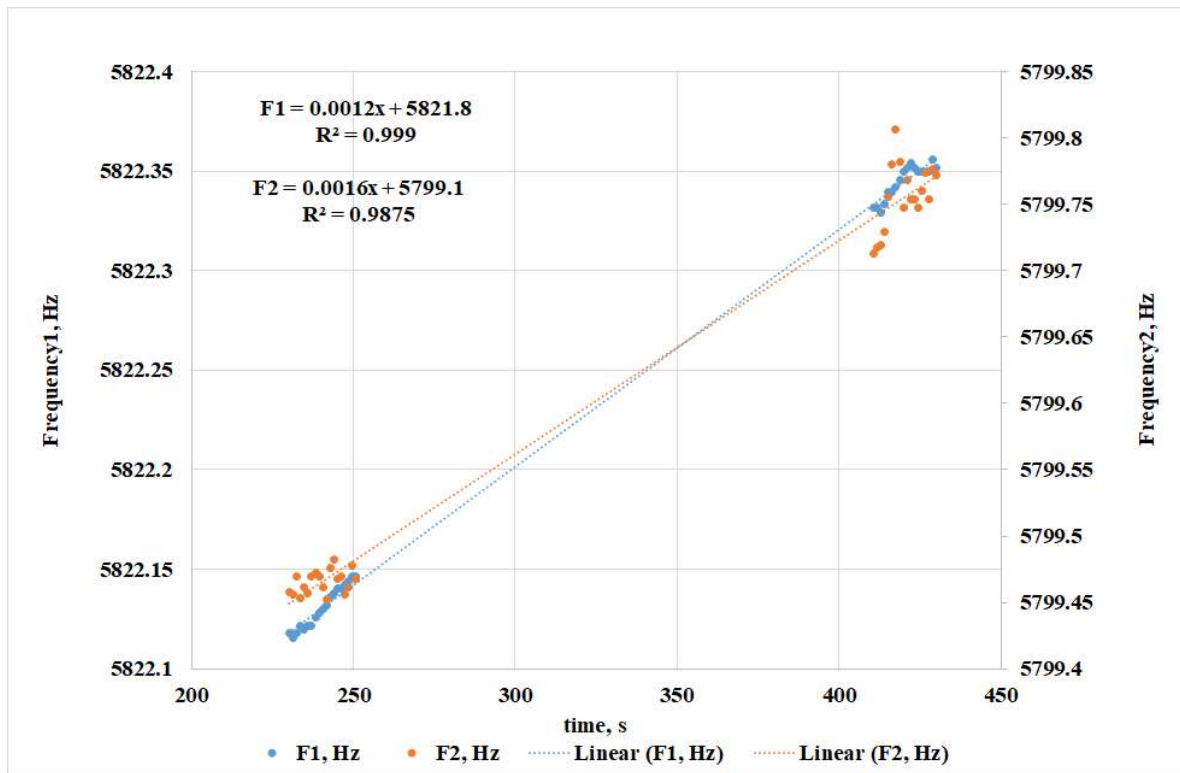


Figure 12. Calculations of the drift parameters.

In order to get rid of the graph drift, a new column should be defined (in new sheet Exp_reco), as shown in Fig. 12, where the drift value at that point were be subtracted from the frequency at each point: $F_i = C_i - (5821.8 + 0.0012 \cdot A_i)$ and $G_i = D_i - (5799.1 + 0.0016 \cdot A_i)$, where parameter i is varied from 2 to number of measurements (in sheet Exp_reco we accumulated 175 measurements).

| | A | B | C | D | E | F | G |
|----|-------------|------------------|-----------|-----------|----------|--------------|--------------|
| 1 | Time, s | Date | F1, Hz | F2, Hz | Pos, mm | F1_drift, Hz | F2_drift, Hz |
| 2 | 230.283379 | 22.08.2022 12:19 | 5822.1178 | 5799.4579 | 30.445 | 0.04145995 | -0.010553406 |
| 3 | 231.4318946 | 22.08.2022 12:19 | 5822.1158 | 5799.4559 | 30.445 | 0.03808173 | -0.014391031 |
| 4 | 232.5813837 | 22.08.2022 12:19 | 5822.1178 | 5799.47 | 30.56375 | 0.03870234 | -0.002130214 |
| 5 | 233.7205027 | 22.08.2022 12:19 | 5822.1219 | 5799.4532 | 30.6825 | 0.0414354 | -0.020752804 |
| 6 | 234.8559048 | 22.08.2022 12:19 | 5822.1199 | 5799.4619 | 30.915 | 0.03807291 | -0.013869448 |
| 7 | 235.9964549 | 22.08.2022 12:19 | 5822.1219 | 5799.4572 | 31.03125 | 0.03870425 | -0.020394328 |
| 8 | 237.1576095 | 22.08.2022 12:19 | 5822.1219 | 5799.47 | 31.03125 | 0.03731087 | -0.009452175 |
| 9 | 238.3073118 | 22.08.2022 12:19 | 5822.126 | 5799.4721 | 31.1525 | 0.04003123 | -0.009191699 |
| 10 | 239.4428092 | 22.08.2022 12:19 | 5822.128 | 5799.47 | 31.27 | 0.04066863 | -0.013108495 |
| 11 | 240.5776765 | 22.08.2022 12:19 | 5822.1301 | 5799.4619 | 31.3875 | 0.04140679 | -0.023024282 |
| 12 | 241.7329828 | 22.08.2022 12:19 | 5822.1321 | 5799.4525 | 31.62125 | 0.04202042 | -0.034272772 |
| 13 | 242.898936 | 22.08.2022 12:19 | 5822.1362 | 5799.4761 | 31.62125 | 0.04472128 | -0.012538298 |
| 14 | 244.0646755 | 22.08.2022 12:19 | 5822.1382 | 5799.4822 | 31.7425 | 0.04532239 | -0.008303481 |
| 15 | 245.2324123 | 22.08.2022 12:19 | 5822.1402 | 5799.468 | 31.8625 | 0.04592111 | -0.02437186 |
| 16 | 246.3850037 | 22.08.2022 12:19 | 5822.1402 | 5799.47 | 31.9825 | 0.044538 | -0.024216006 |
| 17 | 247.5026608 | 22.08.2022 12:19 | 5822.1423 | 5799.4559 | 32.10125 | 0.04529681 | -0.040104257 |
| 18 | 248.6234507 | 22.08.2022 12:19 | 5822.1443 | 5799.4619 | 32.215 | 0.04595186 | -0.035897521 |
| 19 | 249.7626462 | 22.08.2022 12:19 | 5822.1463 | 5799.4781 | 32.44625 | 0.04658482 | -0.021520234 |
| 20 | 250.8955329 | 22.08.2022 12:19 | 5822.1463 | 5799.468 | 32.56375 | 0.04522536 | -0.033432853 |

Figure 12. Columns *F* and *G* show wire frequency shifts taking into account the drift.

Thus, we got the frequency of the wire vibration caused only by laser beam. Since we are interested not in the frequency drop, but in the photon flux measurements, we form the VWM signals by reversing the columns *F* and *G* signs (the laser beam profile is reconstructed in relative units): $H_i = -(F_i - F_{i-2})$ and $I_i = -(G_i - G_{i-2})$, where parameter *i* is varied from 2 to number of measurements (see Fig. 13).

| | A | B | C | D | E | F | G | H | I |
|----|-------------|------------------|-----------|-----------|----------|--------------|--------------|--------------|----------|
| 1 | Time, s | Date | F1, Hz | F2, Hz | Pos, mm | F1_drift, Hz | F2_drift, Hz | signal1 | signal2 |
| 2 | 230.283379 | 22.08.2022 12:19 | 5822.1178 | 5799.4579 | 30.445 | 0.04145995 | -0.010553406 | 0 | 0 |
| 3 | 231.4318946 | 22.08.2022 12:19 | 5822.1158 | 5799.4559 | 30.445 | 0.03808173 | -0.014391031 | 0.003378219 | 0.003838 |
| 4 | 232.5813837 | 22.08.2022 12:19 | 5822.1178 | 5799.47 | 30.56375 | 0.03870234 | -0.002130214 | 0.002757606 | -0.00842 |
| 5 | 233.7205027 | 22.08.2022 12:19 | 5822.1219 | 5799.4532 | 30.6825 | 0.0414354 | -0.020752804 | 2.45485E-05 | 0.010199 |
| 6 | 234.8559048 | 22.08.2022 12:19 | 5822.1199 | 5799.4619 | 30.915 | 0.03807291 | -0.013869448 | 0.003387031 | 0.003316 |
| 7 | 235.9964549 | 22.08.2022 12:19 | 5822.1219 | 5799.4572 | 31.03125 | 0.03870425 | -0.020394328 | 0.002755691 | 0.009841 |
| 8 | 237.1576095 | 22.08.2022 12:19 | 5822.1219 | 5799.47 | 31.03125 | 0.03731087 | -0.009452175 | 0.004149077 | -0.0011 |
| 9 | 238.3073118 | 22.08.2022 12:19 | 5822.126 | 5799.4721 | 31.1525 | 0.04003123 | -0.009191699 | 0.001428719 | -0.00136 |
| 10 | 239.4428092 | 22.08.2022 12:19 | 5822.128 | 5799.47 | 31.27 | 0.04066863 | -0.013108495 | 0.000791316 | 0.002555 |
| 11 | 240.5776765 | 22.08.2022 12:19 | 5822.1301 | 5799.4619 | 31.3875 | 0.04140679 | -0.023024282 | 5.3157E-05 | 0.012471 |
| 12 | 241.7329828 | 22.08.2022 12:19 | 5822.1321 | 5799.4525 | 31.62125 | 0.04202042 | -0.034272772 | -0.000560475 | 0.023719 |
| 13 | 242.898936 | 22.08.2022 12:19 | 5822.1362 | 5799.4761 | 31.62125 | 0.04472128 | -0.012538298 | -0.003261332 | 0.001985 |
| 14 | 244.0646755 | 22.08.2022 12:19 | 5822.1382 | 5799.4822 | 31.7425 | 0.04532239 | -0.008303481 | -0.003862444 | -0.00225 |
| 15 | 245.2324123 | 22.08.2022 12:19 | 5822.1402 | 5799.468 | 31.8625 | 0.04592111 | -0.02437186 | -0.00446116 | 0.013818 |
| 16 | 246.3850037 | 22.08.2022 12:19 | 5822.1402 | 5799.47 | 31.9825 | 0.044538 | -0.024216006 | -0.00307805 | 0.013663 |
| 17 | 247.5026608 | 22.08.2022 12:19 | 5822.1423 | 5799.4559 | 32.10125 | 0.04529681 | -0.040104257 | -0.003836862 | 0.029551 |
| 18 | 248.6234507 | 22.08.2022 12:19 | 5822.1443 | 5799.4619 | 32.215 | 0.04595186 | -0.035897521 | -0.004491914 | 0.025344 |
| 19 | 249.7626462 | 22.08.2022 12:19 | 5822.1463 | 5799.4781 | 32.44625 | 0.04658482 | -0.021520234 | -0.005124879 | 0.010967 |
| 20 | 250.8955329 | 22.08.2022 12:19 | 5822.1463 | 5799.468 | 32.56375 | 0.04522536 | -0.033432853 | -0.003765415 | 0.022879 |

Figure 13 Columns *H* and *I* represent the signals of the first and second wires, respectively.

Since the second wire is shifted relative to the first by about 1 mm, the profile that the second wire provides must be constructed with this shift in mind (cell *J2* in Fig. 14). Column *K* presents the values of column *E* shifted on *J2*: $K_i = E_i + J_2$, where parameter *i* is varied from 2 to number of measurements.

| | A | B | C | D | E | F | G | H | I | J | K |
|----|-------------|------------------|-----------|-----------|----------|--------------|--------------|--------------|----------|-----------|---------------|
| 1 | Time, s | Date | F1, Hz | F2, Hz | Pos, mm | F1_drift, Hz | F2_drift, Hz | signal1 | signal2 | shift, mm | Pos_shift, mm |
| 2 | 230.283379 | 22.08.2022 12:19 | 5822.1178 | 5799.4579 | 30.445 | 0.04145995 | -0.010553406 | 0 | 0 | 0.93 | 31.375 |
| 3 | 231.4318946 | 22.08.2022 12:19 | 5822.1158 | 5799.4559 | 30.445 | 0.03808173 | -0.014391031 | 0.003378219 | 0.003838 | | 31.375 |
| 4 | 232.5813837 | 22.08.2022 12:19 | 5822.1178 | 5799.47 | 30.56375 | 0.03870234 | -0.002130214 | 0.002757606 | -0.00842 | | 31.49375 |
| 5 | 233.7205027 | 22.08.2022 12:19 | 5822.1219 | 5799.4532 | 30.6825 | 0.0414354 | -0.020752804 | 2.45485E-05 | 0.010199 | | 31.6125 |
| 6 | 234.8559048 | 22.08.2022 12:19 | 5822.1199 | 5799.4619 | 30.915 | 0.03807291 | -0.013869448 | 0.003387031 | 0.003316 | | 31.845 |
| 7 | 235.9964549 | 22.08.2022 12:19 | 5822.1219 | 5799.4572 | 31.03125 | 0.03870425 | -0.020394328 | 0.002755691 | 0.009841 | | 31.96125 |
| 8 | 237.1576095 | 22.08.2022 12:19 | 5822.1219 | 5799.47 | 31.03125 | 0.03731087 | -0.009452175 | 0.004149077 | -0.0011 | | 31.96125 |
| 9 | 238.3073118 | 22.08.2022 12:19 | 5822.126 | 5799.4721 | 31.1525 | 0.04003123 | -0.009191699 | 0.001428719 | -0.00136 | | 32.0825 |
| 10 | 239.4428092 | 22.08.2022 12:19 | 5822.128 | 5799.47 | 31.27 | 0.04066863 | -0.013108495 | 0.000791316 | 0.002555 | | 32.2 |
| 11 | 240.5776765 | 22.08.2022 12:19 | 5822.1301 | 5799.4619 | 31.3875 | 0.04140679 | -0.023024282 | 5.3157E-05 | 0.012471 | | 32.3175 |
| 12 | 241.7329828 | 22.08.2022 12:19 | 5822.1321 | 5799.4525 | 31.62125 | 0.04202042 | -0.034272772 | -0.000560475 | 0.023719 | | 32.55125 |
| 13 | 242.898936 | 22.08.2022 12:19 | 5822.1362 | 5799.4761 | 31.62125 | 0.04472128 | -0.012538298 | -0.003261332 | 0.001985 | | 32.55125 |
| 14 | 244.0646755 | 22.08.2022 12:19 | 5822.1382 | 5799.4822 | 31.7425 | 0.04532239 | -0.008303481 | -0.003862444 | -0.00225 | | 32.6725 |
| 15 | 245.2324123 | 22.08.2022 12:19 | 5822.1402 | 5799.468 | 31.8625 | 0.04592111 | -0.02437186 | -0.00446116 | 0.013818 | | 32.7925 |
| 16 | 246.3850037 | 22.08.2022 12:19 | 5822.1402 | 5799.47 | 31.9825 | 0.044538 | -0.024216006 | -0.00307805 | 0.013663 | | 32.9125 |
| 17 | 247.5026608 | 22.08.2022 12:19 | 5822.1423 | 5799.4559 | 32.10125 | 0.04529681 | -0.040104257 | -0.003836862 | 0.029551 | | 33.03125 |
| 18 | 248.6234507 | 22.08.2022 12:19 | 5822.1443 | 5799.4619 | 32.215 | 0.04595186 | -0.035897521 | -0.004491914 | 0.025344 | | 33.145 |
| 19 | 249.7626462 | 22.08.2022 12:19 | 5822.1463 | 5799.4781 | 32.44625 | 0.04658482 | -0.021520234 | -0.005124879 | 0.010967 | | 33.37625 |
| 20 | 250.8955329 | 22.08.2022 12:19 | 5822.1463 | 5799.468 | 32.56375 | 0.04522536 | -0.033432853 | -0.003765415 | 0.022879 | | 33.49375 |

Figure 14. Preparing of column *K* representing transversal axis shifted on value *J2*.

The value of shift is presented in cell *J2* and is subject of fit that provide coinciding of profiles peaks (see Fig. 15).

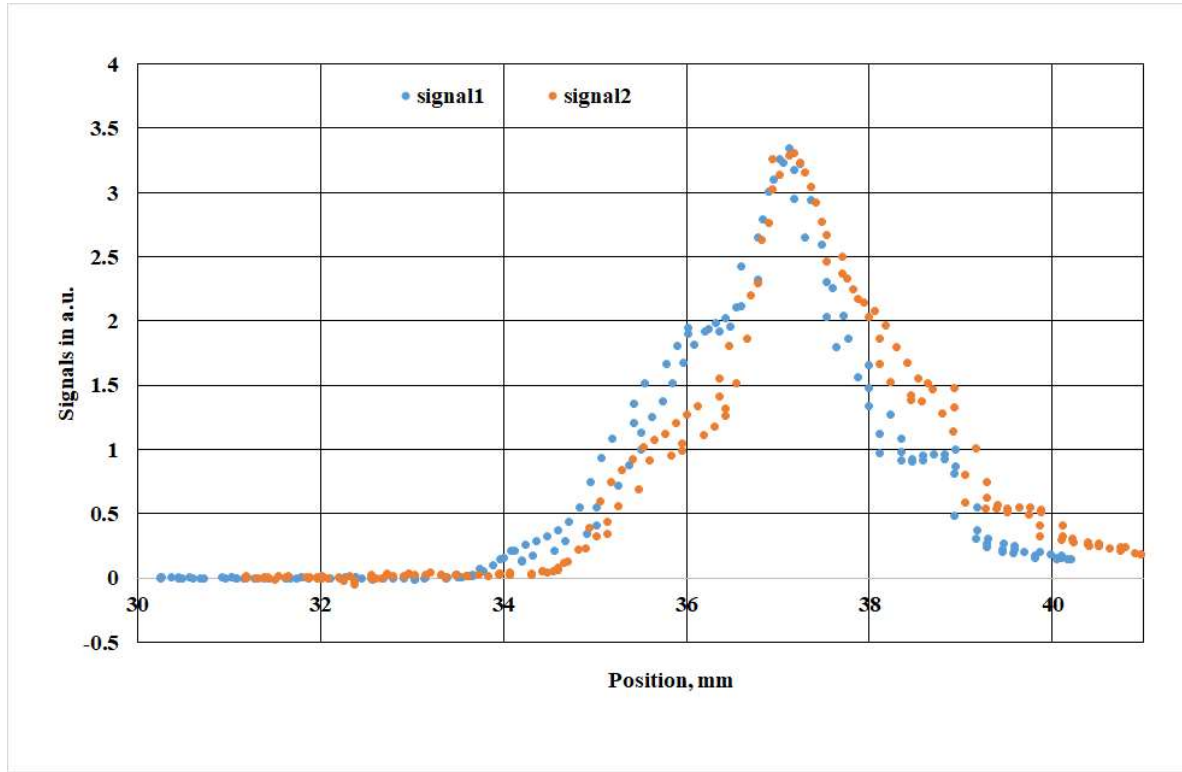


Figure 15. Obtaining of shift parameter by fit of signals from 1st and 2nd wires.

As can be seen from the Fig. 15 the obtained profiles do not coincide as one would expect. This mismatch is due to the following physical effect: each string, in addition to photons of the laser beam, also "sees" reflected photons from another string. Let $P(x)$ be the desired profile of the laser beam, then it is possible to write for the signal which is formed for the first string in the form

$$Signal1 = P(x_1) + K * P(x_2) \quad (1)$$

And the same for second wire:

$$Signal2 = P(x_2) + K * P(x_1). \quad (2)$$

The parameter K determines the number of reradiated photons and should be less than unity.

The process is presented in Fig. 16.

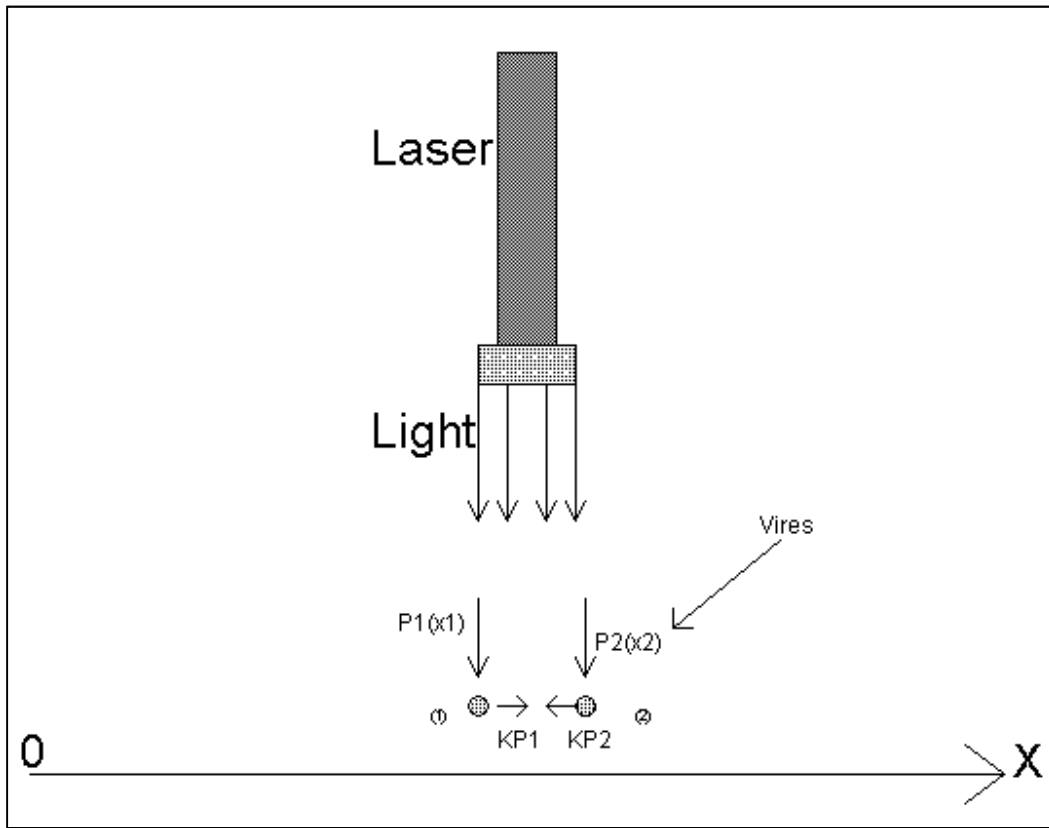


Figure 16: Schematic representation of the process of re-radiation of photons.

From Eqs. 1 and we obtain:

$$P(x_1) = \frac{\text{Signal1}(x_1) - K * \text{Signal2}(x_2)}{1 - K^2}, \quad (3)$$

$$P(x_2) = \frac{\text{Signal1}(x_2) - K * \text{Signal2}(x_1)}{1 - K^2}. \quad (4)$$

| 1 | Time, s | Date | F1, Hz | F2, Hz | Pos, mm | F1_drift, Hz | F2_drift, Hz | signal1 | signal2 | shift, mm | Pos_shift, mm | k | reco1 | reco2 |
|----|-------------|------------------|-----------|-----------|----------|--------------|--------------|--------------|----------|-----------|---------------|------|----------|----------|
| 2 | 230.283379 | 22.08.2022 12:19 | 5822.1178 | 5799.4579 | 30.445 | 0.04145995 | -0.010553406 | 0 | 0 | 0.93 | 31.375 | 0.32 | 0 | 0 |
| 3 | 231.4318946 | 22.08.2022 12:19 | 5822.1158 | 5799.4559 | 30.445 | 0.03808173 | -0.014391031 | 0.003378219 | 0.003838 | | 31.375 | | 0.002395 | 0.003071 |
| 4 | 232.5813837 | 22.08.2022 12:19 | 5822.1178 | 5799.47 | 30.56375 | 0.03870234 | -0.002130214 | 0.002757606 | -0.00842 | | 31.49375 | | 0.006075 | -0.01037 |
| 5 | 233.7205027 | 22.08.2022 12:19 | 5822.1219 | 5799.4532 | 30.6825 | 0.0414354 | -0.020752804 | 2.45485E-05 | 0.010199 | | 31.6125 | | -0.00361 | 0.011354 |
| 6 | 234.8559048 | 22.08.2022 12:19 | 5822.1199 | 5799.4619 | 30.915 | 0.03807291 | -0.013869448 | 0.003387031 | 0.003316 | | 31.845 | | 0.002591 | 0.002487 |
| 7 | 235.9964549 | 22.08.2022 12:19 | 5822.1219 | 5799.4572 | 31.03125 | 0.03870425 | -0.020394328 | 0.002755691 | 0.009841 | | 31.96125 | | -0.00044 | 0.009981 |
| 8 | 237.1576095 | 22.08.2022 12:19 | 5822.1219 | 5799.47 | 31.03125 | 0.03731087 | -0.009452175 | 0.004149077 | -0.0011 | | 31.96125 | | 0.005015 | -0.00271 |
| 9 | 238.3073118 | 22.08.2022 12:19 | 5822.126 | 5799.4721 | 31.1525 | 0.04003123 | -0.009191699 | 0.001428719 | -0.00136 | | 32.0825 | | 0.002077 | -0.00203 |
| 10 | 239.4428092 | 22.08.2022 12:19 | 5822.128 | 5799.47 | 31.27 | 0.04066863 | -0.013108495 | 0.000791316 | 0.002555 | | 32.2 | | -2.9E-05 | 0.002564 |
| 11 | 240.5776765 | 22.08.2022 12:19 | 5822.1301 | 5799.4619 | 31.3875 | 0.04140679 | -0.023024282 | 5.3157E-05 | 0.012471 | | 32.3175 | | -0.00439 | 0.013875 |
| 12 | 241.7329828 | 22.08.2022 12:19 | 5822.1321 | 5799.4525 | 31.62125 | 0.04202042 | -0.034272772 | -0.000560475 | 0.023719 | | 32.55125 | | -0.00908 | 0.026625 |
| 13 | 242.898936 | 22.08.2022 12:19 | 5822.1362 | 5799.4761 | 31.62125 | 0.04472128 | -0.012538298 | -0.003261332 | 0.001985 | | 32.55125 | | -0.00434 | 0.003374 |
| 14 | 244.0646755 | 22.08.2022 12:19 | 5822.1382 | 5799.4822 | 31.7425 | 0.04532239 | -0.008303481 | -0.003862444 | -0.00225 | | 32.6725 | | -0.0035 | -0.00113 |
| 15 | 245.2324123 | 22.08.2022 12:19 | 5822.1402 | 5799.468 | 31.8625 | 0.04592111 | -0.02437186 | -0.00446116 | 0.013818 | | 32.7925 | | -0.0099 | 0.016985 |
| 16 | 246.3850037 | 22.08.2022 12:19 | 5822.1402 | 5799.47 | 31.9825 | 0.044538 | -0.024216006 | -0.00307805 | 0.013663 | | 32.9125 | | -0.0083 | 0.016319 |
| 17 | 247.5026608 | 22.08.2022 12:19 | 5822.1423 | 5799.4559 | 32.10125 | 0.04529681 | -0.040104257 | -0.003836862 | 0.029551 | | 33.03125 | | -0.01481 | 0.03429 |
| 18 | 248.6234507 | 22.08.2022 12:19 | 5822.1443 | 5799.4619 | 32.215 | 0.04595186 | -0.035897521 | -0.004491914 | 0.025344 | | 33.145 | | -0.01404 | 0.029837 |
| 19 | 249.7626462 | 22.08.2022 12:19 | 5822.1463 | 5799.4781 | 32.44625 | 0.04658482 | -0.021520234 | -0.005124879 | 0.010967 | | 33.37625 | | -0.00962 | 0.014045 |
| 20 | 250.8955329 | 22.08.2022 12:19 | 5822.1463 | 5799.468 | 32.56375 | 0.04522536 | -0.033432853 | -0.003765415 | 0.022879 | | 33.49375 | | -0.01235 | 0.026832 |

Figure 17. Columns M and N contains the values obtained from (3) and (4) respectively: $M_i = (H_i - \mathcal{L}\mathcal{L}\mathcal{S}^2 * I_2) / (1 - \mathcal{L}\mathcal{L}\mathcal{S}^2)$ and $N_i = (I_i - \mathcal{L}\mathcal{L}\mathcal{S}^2 * H_2) / (1 - \mathcal{L}\mathcal{L}\mathcal{S}^2)$, where parameter i is varied from 2 to number of measurements.

The parameter K is defined by fit of overlapping of profile reconstructed by Eqs (3) and (4). Best fit is obtained for $K = 0.32$.

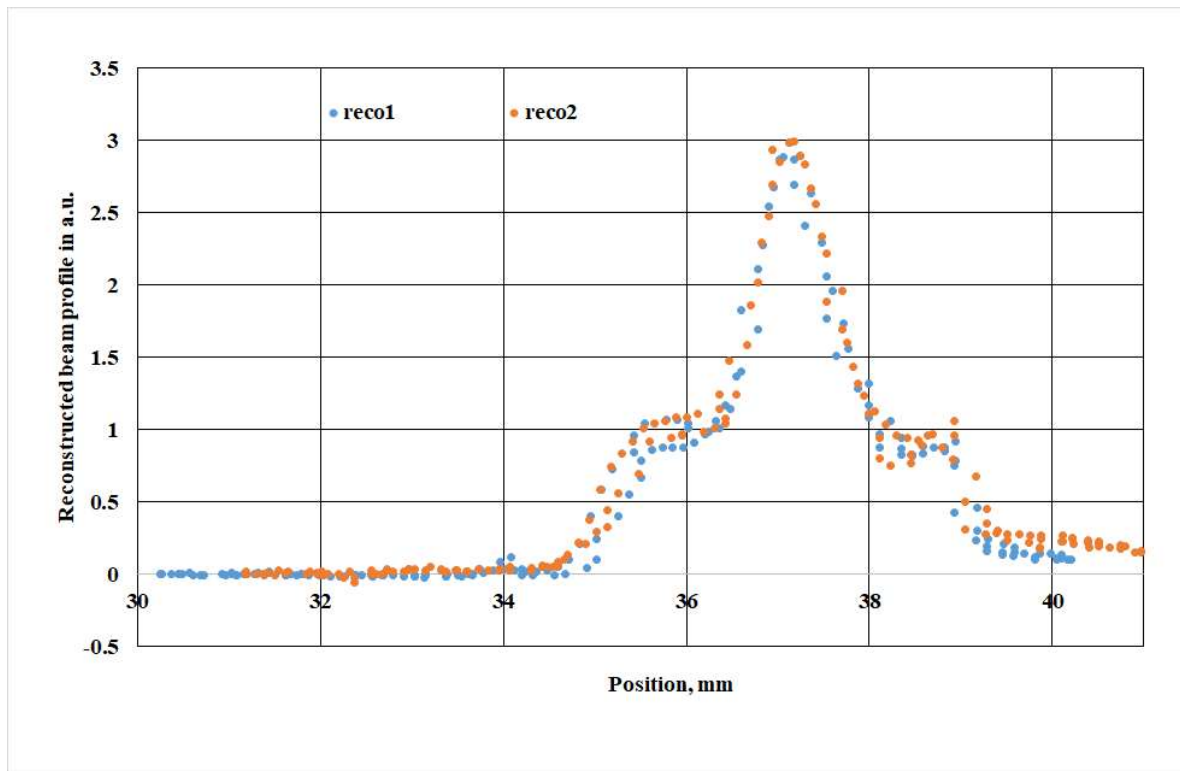


Figure 18. Reconstructed profile with usage the signals from 1st and 2nd wires.

Results of reconstruction of laser beam profile by signals of two vibrating wires are presented in Fig. 18.

Be careful during the experiment

ATTENTION!!!

1. **Make sure that you have completed laser safety training before working with laser.**
2. **Never intentionally look directly into the beam of a laser. Do not stare at the light from any laser. Allow yourself to blink if the light is too bright.**
3. **Do not view a laser with optical instrumentation.**
4. **Never direct the beam toward other people.**
5. **Operate lasers only in the area designed for their use and make sure that the beam is terminated at the end of its use path. Never allow a laser beam to escape its designated area of use.**
6. **Remove all unnecessary reflective objects from the area near the beam's path.**
7. **When working with lasers never wear jewelry or other items which may cause stray reflections.**

Questions

1. Estimate temperature dependence of the frequency of the vibrating wire (Eq. (7) of Practical course: Vibrating wire monitors and beam profile measurements, 2022-4, S.G. Arutunian, E.G. Lazareva, A.V. Margaryan, M.A. Tumanyan).
2. Plot the frequency of vibrating wire and sensitivity of monitor to overheating of wire as functions of temperature of assembly with wires formed of tungsten, beryllium bronze (Beryllium Bronze - Cu97.5/Be2/Co-Ni0.5, UNS C17200), and stainless steel (AISI 316) (Fig. 20 of Practical course: Vibrating wire monitors and beam profile measurements, 2022-4, S.G. Arutunian, E.G. Lazareva, A.V. Margaryan, M.A. Tumanyan).
3. Estimate the temperature shift caused by exposure of the wire to heating power (taking into account thermal transfer through the wire, thermal radiation and convection mechanisms (Eq. (7) of Practical course: Vibrating wire monitors and beam profile measurements, 2022-4, S.G. Arutunian, E.G. Lazareva, A.V. Margaryan, M.A. Tumanyan).
4. Estimate the thermal inertia of the wire (response time). Taking into account thermal transfer through the wire, thermal radiation and convection mechanisms (Eq. (22) of Practical course: Vibrating wire monitors and beam profile measurements, 2022-4, S.G. Arutunian, E.G. Lazareva, A.V. Margaryan, M.A. Tumanyan).

Appendix 1. Detailed description of Soft LabRab

LabRab is a test-bench designed for laboratory works on research of laser beam profile based on vibrating wire sensors.

The general electrical scheme of LabRab is presented in **Fig. 4**.

The LabRab includes an **Arduino Mega 2560** assembly with a 320x240 touchscreen display.

The **Arduino** works in two basic modes-**DUI and PC**:

-**DUI** mode - Standalone LabRab control

-**PC** mode - Computer control of LabRab (Application-VB_Ash_VW_FREQ_v2_2xMotors.exe, hereinafter-**Application**)

The main **Application** forms are shown in **Fig. 4, Fig. 5**.

Arduino operation is performed on three **Frames**:

-**Frame 1** (see **Fig. 1**) - frequency graphs of the 1st and 2nd vibrating wires (hereinafter **F1** and **F2**);

- **Frame 2** (see **Fig. 2**) - the table of parameters **F1, F2**, the direction of movement of the carriage of the linear stepper motor (hereinafter -**Actuator**), the ambient temperature, number of records in ROM;

-**Frame 3** (see **Fig. 3**) - control/settings.

When powering up the LabRab or after resetting the **Arduino (RESET Fig. 1)** - **Frame 3** appears on the screen and the **PC** mode is activated.

- Go to **Frame 1** by clicking on the left-upper section of the display.

- Go to **Frame 2** by clicking on **NEXT** in **Frame 3**.

- Go to **Frame 3** by clicking on the left-bottom section of the display.

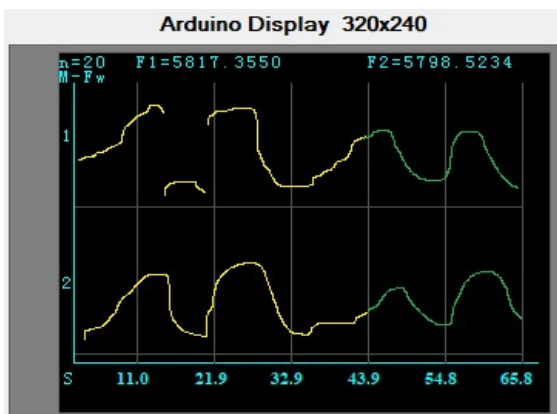


Fig. 1. - Frame 1

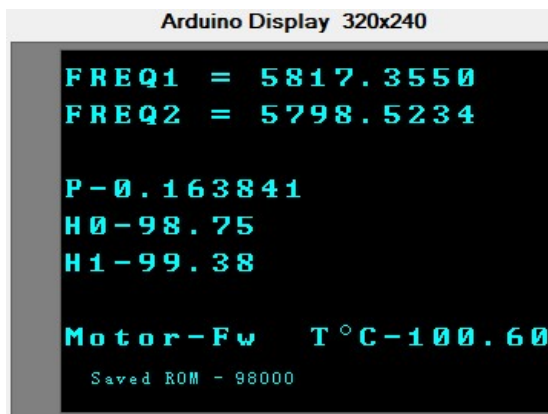


Fig. 2. - Frame 2

FRAME 1 (see Fig.1)

Frame 1 is informational.

Upper sector of the display (1) - Frequency graph **F1**.

Lower sector of the display (2) - Frequency graph **F2**.

n- value of **n(tick)** (see Fig. 3).

M-Fw(Rv) - direction of motion of the **Actuator** carriage.

FRAME 2 (see Fig. 2)

Frame 2 is informational.

FREQ1 - **F1** value, in hertz.

FREQ2 - **F2** value, in hertz.

- P** - Frequency measurement tact, in sec.
- H0** - duration of the positive section of the signal from F1, in μsec .
- H1** - duration of the positive section of the signal from F2, in μsec .
- Motor-Fw(Rv)**- direction of motion of the **Actuator** carriage

FRAME 3 (see Fig. 3)

Frame 3 includes:

- Virtual buttons **-RUN-**, **F****, **Motor Moving**, **DUI**, **Save**, **NEXT** and 4 pairs of "+" and "-" buttons;
- **Led1** and **Led2** are virtual light-emitting diode;



Fig. 3. - Frame 3

n(tick)-value(20), which when multiplied by 0.008192 gives the tact **P** (time in seconds) of measurement of frequencies **F1,F2**;

- **L,mm** - length(10) in mm of cyclic forward(**Fw**) - backward(**Rv**) movement of the **Actuator** carriage;
- **V,mm/s** - speed (0.20) in mm/s of the **Actuator** carriage movement;
- **WPos,mm** - working (initial) position (35) in mm of the **Actuator** carriage.

THE FUNCTION OF THE BUTTONS OF FRAME 3

DUI(PC) - switch of the main modes of LabRab. Each click cyclically takes the value of **PC**, **DUI**. If **Led2** is green, the switch is locked.

- In **PC** mode the master device is **Application**. All buttons are blocked except **DUI(PC)** and **NEXT**.
- In **DUI** mode the master device is **Arduino**.

The graphs and data in **Frames 1** and **2** correspond to the switched on mode (**PC or DUI**).

-RUN- - switches the frequency measurement process on/off.

This automatically changes the color of **Led1**:

- green-on;
- red - off.

- **F**** - at each click cyclically takes the following values: **F****, **F-1**, **F-2**.

- **F****- mode of parallel measurement of frequencies **F1-F2**.

- **F-1** - frequency measurement mode of **F1** only.
- **F-2** - frequency measurement mode **F2** only.

Motor Moving - On/Stop operation of the **Actuator**,

The actuator works in the forward (**Fw**)-backward (**Rv**) cyclic movement mode.

Length of movement and speed are set accordingly by the parameters **L,mm(10)** and **V,mm/s(0.20)**.

- This automatically changes the color of **Led2**:

- green -on;
- red - STOP.

-The **Actuator** also works in the fast working position setting mode (**WPos**).

-The carriage of the **Actuator** first moves backwards to the zero position (triggered by a limit switch), and then forward to the working position **WPos,mm(35)**.

-The **WPos** mode is continued for about 4 seconds. The color of **Led2** changes automatically to blue.

-The **WPos** mode is activated when switching from the carriage cycling mode to the STOP mode. At the end of **WPos** mode **Led2** is set to red.

-WPos mode is also activated after the first start **-RUN-**.

-During the **WPos** mode - all buttons are locked.

NEXT - Goes to **Frame 2**.

"+" and "-" - increase or decrease the corresponding values **N(tick); L,mm; V,mm/s; WPos,mm**.

Save - recording values (parameters) **F**; n(tick); L,mm; V,mm/s; WPos,mm** into permanent memory (ROM) of **Arduino**.

The button is blocked in **PC** mode and when the frequency measurement mode is on (**Led1**-green).

The number of records is fixed in the ROM. Up to 100000 records are allowed for **Arduino**.

The number of recordings is shown in **Frame 2**.

All **Arduino** operating modes work based on the data (parameters)

F; n(tick); L,mm; V,mm/s; WPos,mm**, read from ROM.

Any changes of parameter values without writing them to ROM are invalid

Getting Started Arduino.

1. Switch on the LabRab power supply.
2. Go to **DUI** mode (click on the **PC**).
3. Start the measurement mode (click on **RUN**). Wait for the Actuator carriage to reach **WPos**.
4. Start the **Actuator** (click on **Motor Moving**).
5. Continue as described above (see button functions)

Application and Arduino working together.

- **Application** and **Arduino** must be set to the same basic **DUI/PC** modes.

In **Application** - the modes are switched with the **PC** button (see **Fig. 5**).

- To monitor the processes running from the Arduino, it is necessary in **Application** by clicking on the **READ FREQ** (Fig. 5) and **MOVE** (Fig. 6) buttons.

If the **Application** is not running, it is necessary to disconnect the PC cable from the HUB LAN in LabRab (Fig. 4).

Algorithm of going from one mode to another.

Going from DUI to PC mode:

1. In Arduino click on **DUI (DUI->PC)**;
2. In Application click on **DUI (DUI->PC)**;
3. In Application click on **READ FREQ**.

Going from PC mode to DUI mode:

1. In Arduino click on **PC (PC->DUI)**;
2. In Application click on **PC (PC->DUI)**;
3. Wait until all the processes (messages) in Application are finished;
4. In Application click on **READ FREQ**;
5. In Arduino click on **-RUN-**.

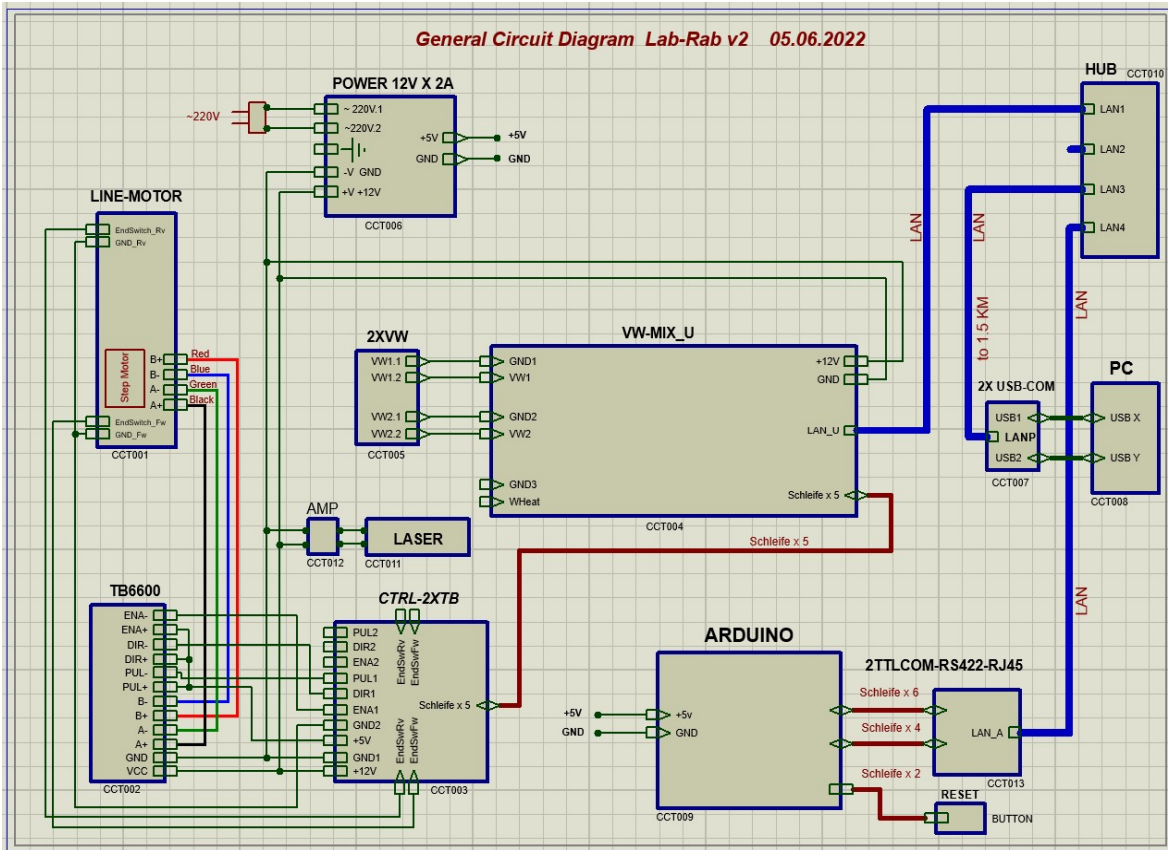


Fig. 4. General Circuit Diagram LabRab

The LabRab circuit includes the following main blocks:

- VW MIX_U-2-** Vibrating wire generation processor board, receive/transmit byte information **F1, F2** and **Actuator** via LAN cable via 2xSerial Port RS232;
- 2xVW-2** wire frequency sensor **F1, F2**;
- Line MOTOR- Actuator**;
- TB6600-Actuator** stepper motor driver;
- CTRL-2xTB-Actuator** control board;
- ARDUINO-Arduino** Mega 2560 assembly with touch screen display (320x240);
- 2TTLCOM-RS422-RJ45** TTL-LAN matching board;
- AMP** voltage amplifier-regulator for Laser (**LASER**);
- PC, 2X USB-COM** dual USB-Serial Port RS232 converter with LAN link (can be up to 1,5 km away from **LabRab**);
- POWER 12V X 2A**-power supply (AC-DC converter 220v AC to 12V x2A DC converter);
- RESET**-Reset the **Arduino**.

Function of the main Application buttons (Fig. 5, Fig. 6).

PC (Fig. 5)-switch of the main PC/DUI modes.

READ FREQ (Fig. 5) - start of the measurement procedure of frequencies F1 and F2.

STOP (Fig. 5) - stop the procedure of measurement of frequencies F1 and F2.

Ch1 and Ch2 (Fig. 5)- resolution of measurement of frequencies F1 and F2 respectively.

MOVE (Fig. 6) - start of movement of the carriage of the Actuator.

STOP (Fig. 6) - stop the movement of the carriage.

RESET (Fig. 6) - resetting the Actuator control board.

Fv (Fig. 6) - direction of carriage movement.

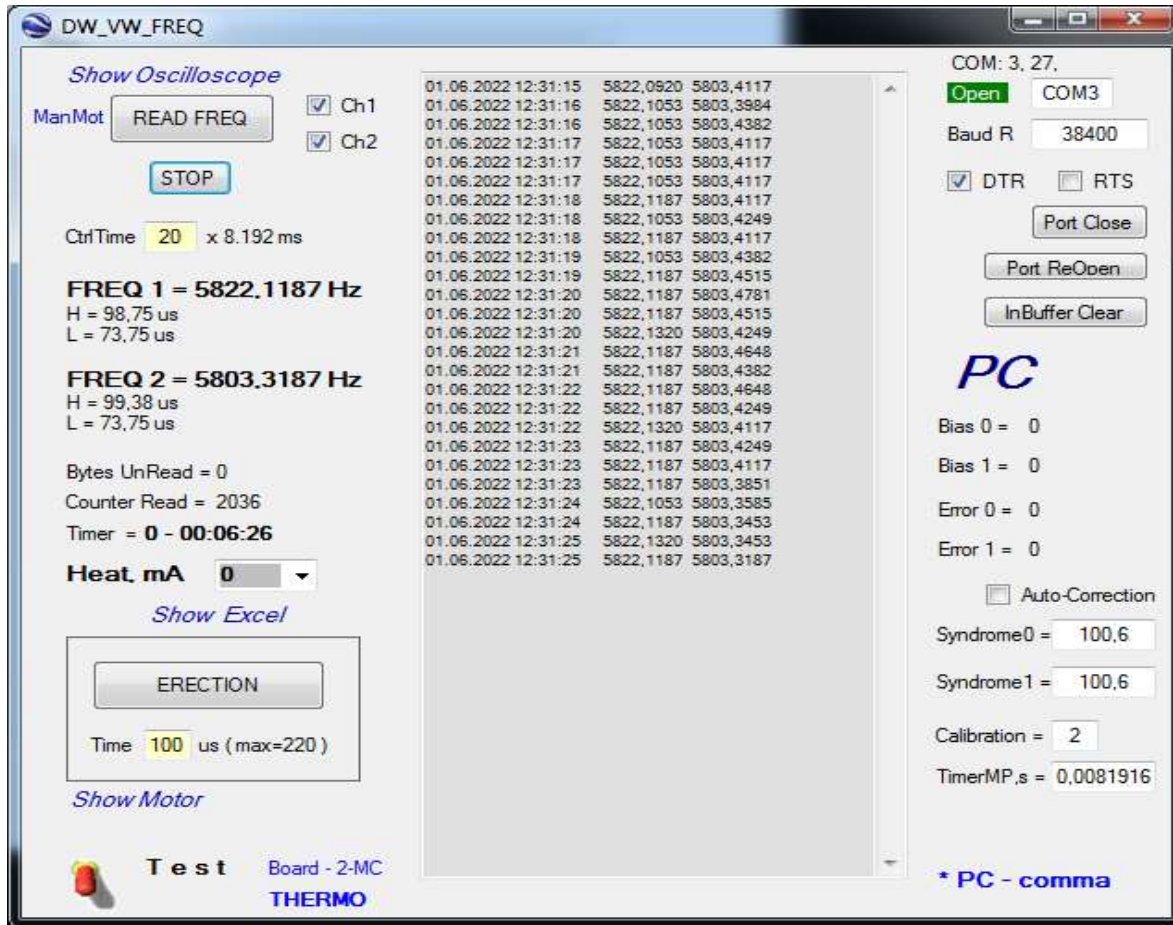


Fig. 5. General Form

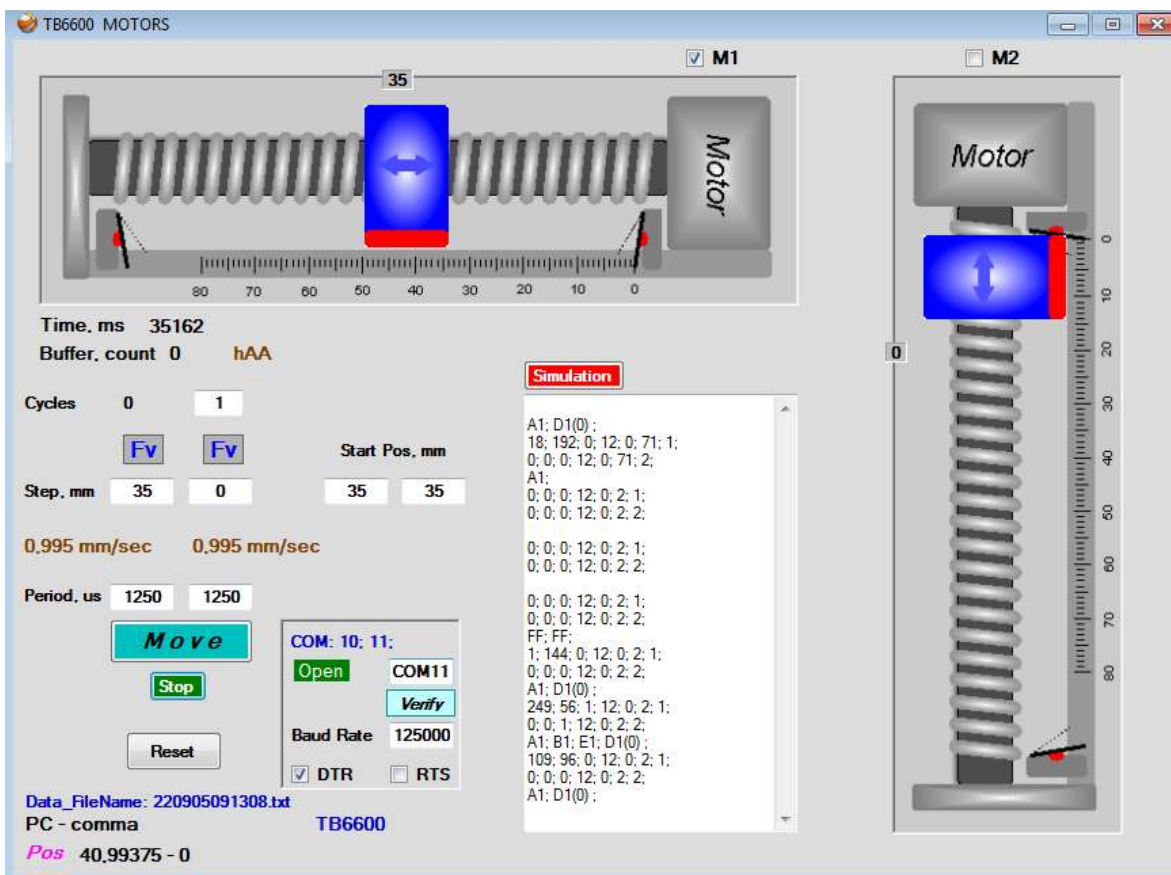


Fig. 6. Actuator